Production and asymmetric fragmentation of multicharged fullerene ions in $Xe^{8+}+C_{60}$ collisions

S. Martin, L. Chen, A. Denis, and J. Désesquelles
Laboratoire de Spectrométrie Ionique et Moléculaire, UMR CNRS No. 5579, Campus de la Doua, Université Lyon 1, 69622 Villeurbanne Cedex, France
(Received 15 January 1998)

The stability of multicharged C_{60}^{q+} $(3 \leqslant q \leqslant 6)$ fullerene ions, produced by slow ($v = 0.2$ a.u.) Xe^{8+}-ion impact, has been studied using coincidence measurements between outgoing projectiles, recoil ion fragments, and ejected electrons. Evidence was found for sequential evaporation of C_{60}^{3+}, for competition between evaporation and fission of C_{60}^{4+}, and for dominant asymmetric fission of C_{60}^{5+} into triply and quadruply charged even-numbered fullerene and low-mass singly charged and neutral carbon clusters. [S1050-2947(98)00606-4]

PACS number(s): 34.70.+e, 36.40.-c, 82.30.Fi

Properties of multicharged clusters have received much attention in recent years [1]. For a given charge state, the stability depends on the cluster size. For a given size, the critical charge is reached when the repulsive Coulomb energy amounts to the total binding energy. It defines the limit of the observability of kinetically stable charged clusters, above which clusters will decay spontaneously in an explosion that presents similarities to the Coulomb instability of nuclei [2,3]. The observation of highly charged clusters and molecules is not uncommon. Among them, fullerene ions are particularly stable. The critical charge of C_{60} has been found to be about $q = 16$ in quantum molecular-dynamics calculations [4]. Such a high value has not been experimentally confirmed yet. However, the observation of C_{60}^{q+} with q up to 7 and 9, under electron [5] and ion [6,7] impact, respectively, has shown the high stability of C_{60} against a Coulomb explosion.

A number of recent studies have shown that the dissociation dynamics of multiply charged clusters is controlled by excess energy in the precursor cluster and, for small systems, by the detailed initial geometric configuration. The cluster charge and size dependence of fragmentation channels has been analyzed mainly in photoexcitation experiments [8] and the classical charged droplet model [9] often has been used to explain the competition between the evaporation of neutral small fragments and Coulomb fission into charged products.

Fragmentation of C_{60} has been studied in photofragmentation experiments by O'Brien *et al.* [10]. Many findings on singly and multiply charged fullerene fragmentation have been established in crossed electron C_{60} vapor beam experiments [11]. Evaporation and asymmetrical fission have been observed for fullerene ions up to C_{60}^{7+} [5]. Measured kinetic energies of C_2^+ fission products of C_{60}^{q+} $(3 \leqslant q \leqslant 6)$ have been explained by a double step reaction composed of evaporation of C_2 and charge transfer from the heavy fullerene ion onto the neutral fragment [12]. A more recent approach to the study of fullerene ionization and fragmentation consists in analyzing products of collisions between accelerated C_{60}^{q+} beams and gas targets [13] or between multicharged ion beams and fullerene targets [6,14,15]. In such collisions, highly charged C_{60}^{q+} ions can be observed because the energy released in the charged fullerene could be much lower than in the photo- and electron-induced ionizations where stable clusters are limited to lower charge states.

In this paper we report studies of C_{60}^{q+} produced in $Xe^{8+}+C_{60} \rightarrow Xe^{(8-s)+}+C_{60}^{q+}+(q-s)e^-$ single collisions at 128 keV by electron capture processes. To get maximum intensities of C_{60}^{q+} around $q = 3-5$, only collision events with the stabilization of two electrons to the projectiles ($s = 2$) have been investigated. C_{60}^{q+}, referred to as a ''parent ion,'' can dissociate into charged and neutral fragments. By coincident measurements of scattered projectile Xe^{6+}, recoil ion fragments, and autoionized electrons, we have studied the unimolecular dissociation mechanisms of C_{60}^{q+} $(q = 3-5)$. An evolution of the competition between evaporation and fission channels is presented as a function of the parent ion C_{60}^{q+} charge state.

Xe^{8+} projectile ions from the electron cyclotron resonance (ECR) ion source of accélérateur d'ions multichargés (AIM) facility at Grenoble were accelerated to 128 keV, collimated to a beam of a few nanoamperes, 1 mm or less in diameter, and then intercepted perpendicularly by a thermal fullerene molecular beam. Powder containing 99.9% C_{60} and 0.1% C_{70} was evaporated in an oven at 520 °C and the vapor was introduced in the interaction region through a 1-mm-diam orifice. The pressure in the reaction chamber was about 5×10^{-6} mbar during operation. The outgoing projectiles were charge selected by a cylindrical electrostatic analyzer ($R = 150$ mm) and detected by a channeltron electron multiplier. Recoil ions and ejected electrons were extracted from the interaction region by a transverse homogeneous electric field of 600 V/cm. The mass and charge state of C_{60}^{q+} ions and C_m^{p+} fragments were determined by a time of flight (TOF) spectrometer ($l = 120$ mm). The use of several meshes ($\simeq 90\%$ transmission each) along the TOF tube limits the recoil ion collection ratio to about 30%. Collected recoil ions were postaccelerated to 7 kV in front of a multichannel plate (MCP) detector in order to increase the detector efficiency for monocharged fullerenes and fragments. On the other side, the extracted electrons were accelerated towards a semiconductor detector (passivated implanted planar silicon detector, $S = 150$ mm^2) biased at 20 kV. An intermediate electrode, set at 2 kV, has been used to collect all electrons ejected inside the interaction region with energies less than the Xe^{8+} potential energy of 106 eV that limits the energy of autoionized electrons. The amplitude of the electron signal is a measure of the number of emitted electrons. It was ampli-

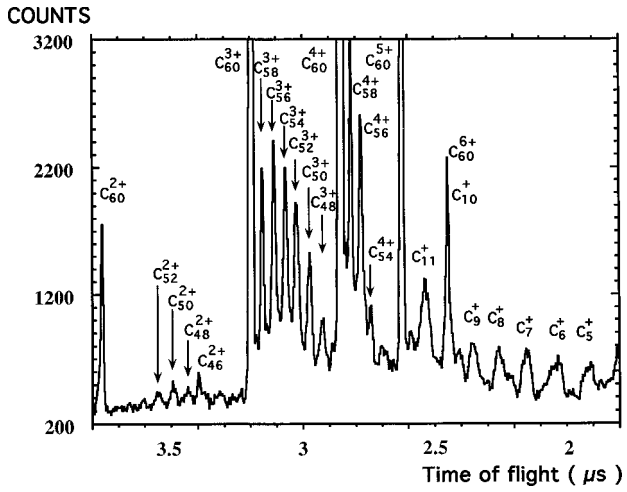

FIG. 1. TOF spectrum of recoil ions from Xe^{8+} on C_{60} collisions when projectile ions have stabilized two electrons. Evaporation and/or asymmetrical fission of C_{60}^{3+}, C_{60}^{4+}, and C_{60}^{5+} produce neighboring C_{58-48}^{3+} and C_{58-54}^{4+} peaks. C_5^+ to C_{11}^+ peaks result from ''multifragmentation'' into several small fragments.

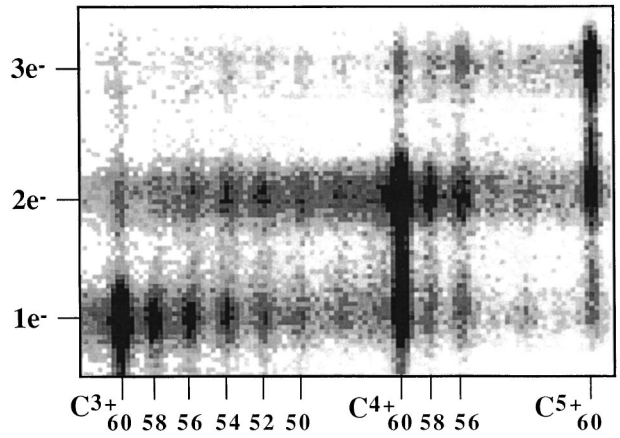

FIG. 2. Electron recoil ion TOF 2D spectrum registered in coincidence with Xe^{6+}. The pulse height of the electron detector is plotted on the Y axis and the TOF of recoil ions is plotted on the X axis. The spots $1e^-$-C_{60}^{4+} and $2e^-$-C_{60}^{5+} result, respectively, from the spots $2e^-$-C_{60}^{4+} and $3e^-$-C_{60}^{5+} due to the electron backscattering effect.

fied, delayed, and sent to a grounded analog to digital converter (ADC) through a fiber optics transmission system for pulse height analysis. The probability for electrons to release the totality of their 20 keV energy inside the detector is equal to 83%. The missing 17% is attributed to backscattered electrons that release only a part (about 12 keV) of their energy inside the detector. Triple coincidence measurements were performed as follows. A channeltron signal due to a Xe^{6+} scattered ion was suitably delayed (8 μs). It was used as trigger for delayed electron pulse height ADC conversion and gave a common stop signal to a multihit time to digital converter for which recoil ion fragment signals provided start pulses.

In Fig. 1 we present a simple recoil ion TOF spectrum in coincidence with the detection of Xe^{6+} ions. The strong intensity of C_{60}^{q+} $(2 \leqslant q \leqslant 6)$ peaks shows the stability of multicharged clusters produced in such collisions. They are attributed, similarly to ion-atom collisions, to stabilized double capture, triple capture followed by autoionization of one electron, doubly autoionizing quadruple capture, and so on [16,17]. The heavy, multicharged C_{60-2n}^{p+} $(2 \leqslant p \leqslant 5,\ 1 \leqslant n \leqslant 5)$ ion peaks are more interesting. They result from the dissociation of different multiply ionized C_{60} fullerenes that have obtained enough internal energy during the collisions. Their low intensities relative to the C_{60}^{q+} ions suggest that only a small part of C_{60}^{q+} prepared in such collisions is dissociated in the time of flight of the extraction region. However, from this spectrum, we cannot identify precisely the parent ion for each fragment. For example, it may be asked whether the C_m^{3+} peaks were issued from the neutral fragment evaporation of C_{60}^{3+} or from the asymmetric fission of C_{60}^{4+}.

This question has been resolved by analyzing the number of electrons autoionized in each collision event. By the charge conservation, the initial charge of C_{60} is deduced by the number of autoionized electrons plus the two electrons stabilized to the projectile. In Fig. 2 we present a two-dimensional (2D) scatter, electron-recoil ion TOF spectrum registered by plotting the pulse height of the electron detector signal along the vertical Y axis and the time of flight of related recoil ions along the horizontal X axis. From partial X projections of this spectrum, we can select recoil ion TOF spectra in coincidence with the detection of one, two, and three electrons. After correction for electron backscattering effects [18], we have obtained the three TOF spectra [Figs. 3(a), 3(b), and 3(c)] associated with C_{60}^{3+}, C_{60}^{4+}, and C_{60}^{5+} parent ions, respectively. The intensities of fragments and C_{60}^{3+}, C_{60}^{4+}, and C_{60}^{5+} ions are listed in Table I. The relative intensities of C_{60}^{3+}, C_{60}^{4+}, and C_{60}^{5+} in Table I were found to be in good agreement with those in Fig. 1, showing that the efficiency of the optics guiding the ejected electrons to the detector is sufficient in this experiment.

TABLE I. Size and charge distribution of evaporation and asymmetric fission fragments of multiply charged C_{60} clusters.

		Parent multiply charged clusters		
Fragments		C_{60}^{3+}	C_{60}^{4+}	C_{60}^{5+}
C_m^{2+}	52	60		
	50	90		
	48	70		
C_m^{3+}	60	7900		
	58	1450	110	
	56	1100	470	50
	54	590	670	160
	52	270	740	150
	50	130	370	160
	48		240	80
C_m^{4+}	60		11000	
	58		1000	210
	56		470	400
	54			140
C_m^{5+}	60			1800
	58			50

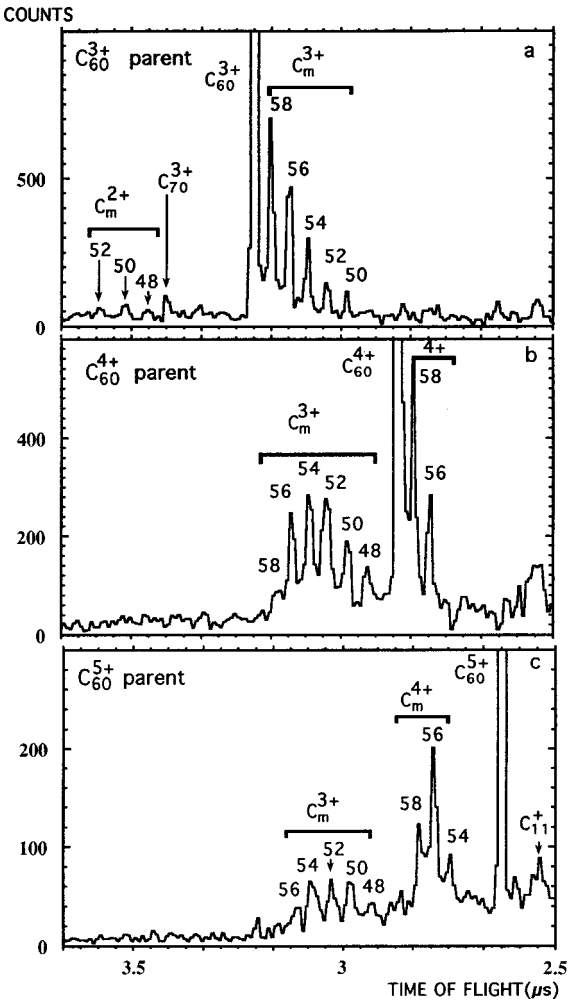

FIG. 3. Recoil ion TOF spectra in coincidence with the detection of (a) one, (b) two, and (c) three electrons obtained by partial X projections of the 2D spectrum (Fig. 2) after correction for the electron backscattering effect. (a) For C_{60}^{3+} parent ions, evaporation is the dominant process. (b) For C_{60}^{4+}, there is a competition between evaporation and fission processes. (c) For C_{60}^{5+}, asymmetrical fission is dominant.

The intense C_{60-2n}^{3+} $(n=1-5)$ peaks of Fig. 3(a) were unambiguously produced by the evaporation of C_2 clusters, whereas the weak C_{60-2n}^{2+} $(n=4-6)$ ones were clearly due to asymmetric fission of the C_{60}^{3+} parent ions. It is not surprising to find that the evaporation is the prevailing decay channel, as it is predictable by applying the classical droplet model [9] to C_{60}^{3+}, which presents a high fission barrier. From the measured C_{60-2n}^{3+} intensity distribution, we deduced an internal energy of 60 ± 15 eV for the C_{60}^{3+} parent ion by using the model of unimolecular reactions [19]. The TOF spectrum with parent ions C_{60}^{4+} [Fig. 3(b)] presents two groups of peaks with comparable intensities. C_m^{4+} $(m=58,56)$ results from evaporation of C_2 clusters, whereas C_m^{3+} $(m=58-48)$ results from asymmetric Coulomb fission. So fission channels become as important as evaporation channels in this case. In collisions giving C_{60}^{5+} parent ions [Fig. 3(c)], the essential reaction route is the asymmetric fission to C_m^{4+} $(m=58,56,54)$ and low-mass singly charged ions. The C_m^{3+} $(m=56-48)$ series can be explained as resulting from asymmetric fissions with emission of two singly charged small fragments.

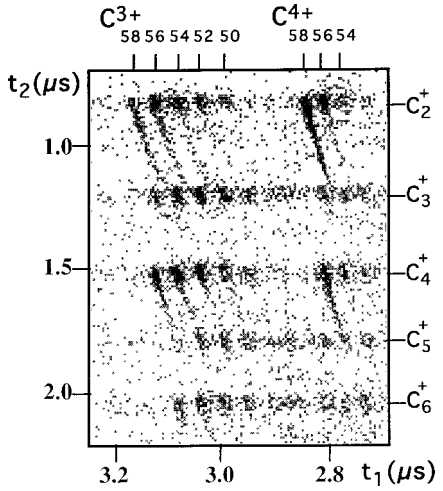

FIG. 4. Correlated recoil ion 2D spectrum: the time of flight t_1 of the last detected fragment (the heaviest one) versus the time of flight t_2 of the correlated small C_m^+ fragments. The tails prolonging some spots are due to delayed fission of C_{60}^{4+} and C_{60}^{5+} during the extraction time.

The analysis of a fission process, in which at least two charged fragments are issued from a parent ion, could be completed by studying the correlation between these fragments. In Fig. 4 we present a 2D spectrum where the horizontal axis represents the time of flight of the last detected (heaviest) fragment and the vertical axis gives the time of flight of other fragments associated with the same collision event. This spectrum, taken without selecting the number of electrons, shows the correlations between heavy- and low-mass charged fragments arising mainly from C_{60}^{4+} and C_{60}^{5+} parent ions. The intense C_{58}^{4+}-C_2^+ spot, located on the right-hand side of Fig. 4, is attributed to the fission channel $C_{60}^{5+}\rightarrow C_{58}^{4+}+C_2^+$. It corresponds to the strong C_{58}^{4+} peak of Fig. 3(c). The long oblique tail that prolongs the spot towards shorter flight times of C_{58}^{4+} and longer flight times of C_2^+ is due to delayed dissociation of C_{60}^{5+} ions all along their path between the extraction plates. The flight time of the C_{58}^{4+} produced by delayed fission of C_{60}^{5+} is shorter than the nominal flight time of the primary C_{58}^{4+} ions and the associated C_2^+ fragments are slower than the primary C_2^+. The slope of the tail is well reproduced by calculations from mass and charge ratios and the intensity variation along the tail gives an estimated decay time of the order of 100 ns. A similar explanation applies to the tails of other spots. The C_{56}^{4+}-C_4^+ and C_{56}^{4+}-C_2^+ spots show that C_{56}^{4+} ions are produced by fission of C_{60}^{5+} via two different channels giving rise either to C_4^+ or to C_2^+ and C_2. The weakness of the C_{54}^{4+}-C_4^+ spot and the absence of the C_{54}^{4+}-C_6^+ spot indicate that the weak C_{54}^{4+} peak of Fig. 3(c) corresponds to the evaporation of a C_2 dimer by C_{60}^{5+} followed by the fission of C_{58}^{5+} into C_{54}^{4+} and C_4^+.

The spots appearing on the left-hand side of the correlation spectrum associate C_{60-2n}^{3+} fullerene ions with low-mass singly charged fragments. They largely arise from the fission of C_{60}^{4+}. The weak C_{58}^{3+}-C_2^+ spot reflects the small C_{58}^{3+} peak of Fig. 3(b). The intense C_{56}^{3+}-C_4^+ spot represents an important fission channel of C_{60}^{4+} leading to the

strong C_{56}^{3+} peak in Fig. 3(b). However, the observation of C_{56}^{3+}-C^{+} (not shown in the figure), C_{56}^{3+}-C_2^{+}, and C_{56}^{3+}-C_3^{+} spots demonstrates that other dissociation channels producing more than two low-mass fragments, neutral as well as ionized ones, are also associated with the C_{56}^{3+} peak. Similarly, numerous spots corresponding to correlations between C_{54}^{3+} and several low-mass fragments C_m^{+} $(m=2-5)$ show that the C_{54}^{3+} peak in Fig. 3(b) is assigned to several dissociation channels producing more than two low-mass fragments including small neutral clusters, but not to the simplest fission way $C_{54}^{3+}+C_6^{+}$.

In conclusion, we have investigated the fragmentation of charged C_{60}^{q+} ions $(q=3-5)$ produced by a collision between a highly charged ion beam and a C_{60} molecular jet by using triple-particle coincidence measurements between outgoing projectile charge states, electrons, and mass analyzed target fragments. In the case of a large impact parameter, highly charged C_{60}^{q+} ions have been observed. The decay channels of C_{60}^{q+} are very different, depending on the initial parent ion charge state. C_{60}^{3+} decays dominantly by evaporation of small even-numbered neutral clusters. Its initial energy is estimated as about 60 eV. C_{60}^{5+} decays by asymmetric fission with production of a charged fullerene and low-mass neutral and charged carbon fragments. For C_{b60}^{4+}, there is a competition between evaporation and asymmetric fission showing the existence of a critical charge state for C_{60}^{q+} in the decay processes. Several asymmetric fission channels have been observed for a selected parent ion C_{60}^{4+} or C_{60}^{5+}. The recoil ion correlation spectrum gives information on fission fragments and lifetimes of different decay channels. Similar results have been obtained by Scheier *et al.* [12] on the strong charge dependence of the branching ratio for evaporation and fission channels. However, they studied the decays of metastable (several microseconds to several 10^{-5} s) C_{60}^{q+} states produced by electron impact. We quantitatively studied faster decay processes (~100 ns) of more excited C_{60} ions produced by highly charged ion impact. The similarity of results obtained in both experiments shows that the competition between evaporation and fission does not depend too much on the initial internal energy of C_{60}.

Discussions with M. Broyer, Ph. Dugourd, J. Lermé, and M. Pellarin are gratefully acknowledged. The authors would also like to acknowledge A. Brenac at CEA-Grenoble for supplying ion beams used in these experiments. LASIM is Unité de Recherche de l'Université de Lyon et du CNRS No. 5579.

[1] O. Echt and T. D. Märk, in *Clusters of Atoms and Molecules*, edited by H. Haberland, Springer Series in Chemical Physics Vol. 52 (Springer-Verlag, Berlin, 1994), Vol. II, p. 183.
[2] C. Brechignac, Ph. Cahuzac, F. Carlier, M. de Frutos, J. Laygnier, and A. Scarfati, Phys. Rev. B **44**, 11 386 (1991).
[3] F. Chandezon *et al.*, Phys. Rev. Lett. **74**, 3784 (1995).
[4] G. Seifert, R. Gutierrez, and R. Schmidt, Phys. Lett. A **211**, 357 (1996).
[5] P. Scheier and T. D. Märk, Phys. Rev. Lett. **73**, 54 (1994).
[6] J. Jin, H. Khemlich, M. H. Prior, and Z. Xie, Phys. Rev. A **53**, 615 (1996).
[7] B. Walch, C. L. Cocke, R. Völpel, and E. Salzborn, Phys. Rev. Lett. **72**, 1439 (1994).
[8] C. Brechignac *et al.*, in *Large Clusters of Atoms and Molecules*, edited by T. P. Martin (Plenum, New York, 1995), p. 315.
[9] C. Brechignac, Ph. Cahuzac, F. Carlier, M. de Frutos, J. Leygnier, and J. Ph. Roux, J. Chem. Phys. **102**, 763 (1995).
[10] S. C. O'Brien, J. R. Heath, R. F. Curl, and R. E. Smalley, J. Chem. Phys. **88**, 220 (1988); see also H. Hohmann *et al.*, Phys. Rev. Lett. **73**, 1919 (1994).
[11] T. D. Märk and P. Scheier, Nucl. Instrum. Methods Phys. Res. B **98**, 469 (1995).
[12] P. Scheier, B. Dünser, and T. D. Märk, Phys. Rev. Lett. **74**, 3368 (1995).
[13] P. Hvelplund, L. H. Andersen, C. Brink, D. Y. Yu, D. C. Lorents, and R. Ruoff, Z. Phys. D **30**, 323 (1994); and P. Hvelplund *et al.*, Phys. Rev. Lett. **69**, 1915 (1992).
[14] N. Selberg *et al.*, Phys. Rev. A **53**, 874 (1996).
[15] S. Cheng *et al.*, Phys. Rev. A **54**, 3182 (1996).
[16] S. Martin, J. Bernard, L. Chen, A. Denis, and J. Désesquelles, Phys. Rev. A **52**, 1218 (1995).
[17] S. Martin, J. Bernard, L. Chen, A. Denis, and J. Désesquelles, Phys. Scr. **T73**, 149 (1997).
[18] F. Aumayr, G. Lakits, and H. Winter, Appl. Surf. Sci. **47**, 139 (1991).
[19] W. Forst, *Theory of Unimolecular Reaction* (Academic, New York, 1973), p. 68.